UCRL- 93191
PREPRINT

Zone Plate Imaging of 14-MeV Neutrons

R. A. Lerche, S. M. Lane,
A. M. Hawryluk, and N. M. Ceglio

This Paper was Prepared for Submittal to
the Proceedings for the 7th International
and Related Plasma Phenomena
Monterey, CA
10/28-11/1/85

4/1/86

Lawrence Livermore National Laboratory

DISCLAIMER

Zone Plate Imaging of 14-MeV Neutrons*

R. A. Lerche, S. M. Lane, A. M. Hawryluk and N. M. Ceglio
University of California
Lawrence Livermore National Laboratory
Livermore, California 94550 USA

INTRODUCTION

At Livermore we are interested in imaging the thermonuclear burn region of fusion targets irradiated at our Nova laser facility. We expect compressed core diameters to be 10's of microns, and would like images with better than 10-μm resolution. Alpha particle images provided the first direct information about the thermonuclear burn geometry in thin walled exploding pusher targets [1]. In future high density target experiments, only highly penetrating radiations like the 14-MeV neutrons will escape the target core to provide information about the burn region [2]. To make the measurement with a neutron "pinhole" camera requires a 10-μm pinhole through about 10 cm of material and 10^{14} to 10^{15} source neutrons [3]. Penumbral imaging offers some improvement over a pinhole [7].

Zone plate coded imaging (ZPCI) techniques are particularly well suited for imaging small objects like the compressed core of a laser fusion target. We have been using ZPCI techniques to image nonpenetrating radiations like x rays and alpha particles for about 10 years [4]. The techniques are well developed.

*Work performed under the auspices of the U. S. Department of Energy by the Lawrence Livermore National Laboratory under contract number W-7405-ENG-48.

Imaging penetrating radiations like 14-MeV neutrons using ZPCI techniques has several possible advantages. The large solid angle subtended by the zone plate might substantially reduce the required target neutron yield needed to produce a useful image, and a neutron zone plate system with 10-μm resolution might be easier to fabricate and characterize than a pinhole system. This paper explores the use of ZPCI techniques with penetrating radiation.

ZONE PLATE CODED IMAGING

Figure 1 illustrates the basic principles of zone plate coded imaging. In this two step process a coded image is formed by letting a source of incoherent radiation cast a geometrical shadow of a Fresnel zone plate [5] onto an image plane. In this example three point sources cast three overlapping images of the zone plate onto the image plane. The location of the different sources is encoded by the size and location of the respective shadows. Emissions close to the zone plate cast larger shadows, those off axis to one side produce shadows to the other side. The shadow intensity is proportional to the source strength. The coded image is the convolution of the source distribution with the coded aperture transmission function.

The coded image or shadowgraph is typically processed to create an optical transparency which produces an optical image of the original source when illuminated with coherent light. Here diffraction plays a dominant role. The zone plate provides its unique contribution to the encoding/decoding process in that when illuminated by a coherent light, a zone plate produces a focused spot with an axial position dependent on the size of the coded image. Here the coherent diffraction process performs a Fresnel transform on the shadowgraph pattern. This serves to unfold the source-aperture convolution achieved in the creation of the coded image.

Figure 2 illustrates a neutron zone plate system. The zone plate is a section of a set of concentric right circular cones with a common apex at the center of the source distribution. It is characterized by the source to zone plate distance S_1, the zone plate to detector distance S_2, the detector efficiency η_{det}, and the zone plate characteristics: thickness D, number of zones N, outer zone width ΔR_N, and macroscopic cross sections for the "transparent" and "opaque" zones Σ_t and Σ_o.

A neutron zone plate differs from the ideal zone plate in three significant ways: it's thick, it's tapered, and it has poor signal modulation. A free standing zone plate used in our laser-fusion program with nonpenetrating radiation is typically 15-μm thick and has totally transparent and totally opaque zones. To cast a zone plate shadow with penetrating radiation the opaque zones must attenuate the radiation enough to create modulation in the detector plane. For 14-MeV neutrons this requires the zone plate to be several centimeters thick. For such a thick zone plate, the open or "transparent" zones might need to be filled with a solid material for support and ease of construction. For example, vacuum evaporation techniques might allow construction with in-situ characterization. In this method alternate layers of "opaque" and "transparent" materials would be evaporated onto a rotating cylinder [6]. Material selection for a neutron zone plate should minimize the neutron cross section in the "transparent" zones and maximize it in the "opaque" zones.

The zone boundaries of a thick, tapered zone plate cast sharp shadows for point sources near the zone plate focus (apex of cones). The imaged boundaries between "transparent" and "opaque" zones appear fuzzy for point sources away from the zone plate focus. (See figure 3.) For source points near the focus, the neutron zone plate system achieves coded image sharpness similar to a system with a thin zone plate. For such images standard reconstruction techniques may be applied.

Signal modulation for a neutron zone plate is much poorer than for an ideal zone plate. Instead of totally transparent and totally opaque zones, the "transparent" zones cause some source attenuation and the "opaque" zones allow some transmission. This results in a lower system signal to noise ratio. The following sections discuss the effect of modulation and "fuzzy" boundaries.

MODULATION

Zone plate system signal to noise ratio (SNR) depends on the modulation of the zone plate transfer function. It is readily calculated for a thin zone plate system by dividing the expression for the reconstructed signal by the expression for the standard deviation of the signal. The signal depends only on the coded image events that pass through the "transparent" zones while the standard deviation depends on all events recorded in the coded image. This SNR is also valid for sources near the focus of a thick zone plate system. Rearranging the SNR equation gives an equation for the source strength required to produce an image. The required source strength to produce an image depends on the desired signal to noise ratio, the system dimensions, the detector efficiency, the ZP materials, and the source spatial distribution. The number of events needed in the i^{th} source resolution element may be written as

$$N_o^i = \left(\frac{\pi}{2\sqrt{2}}\right)^2 (SNR)^2 \left(\frac{4S_1}{d_{ZP}}\right)^2 \frac{1}{\eta_{det}} \left(\frac{2}{P_t}\right) \frac{(1+f)}{(1-f)^2} \left(\frac{N_o}{N_o^i}\right) \quad (1)$$

Here d_{ZP} is the diameter of the zone plate, η_{det} is the detector efficiency, P_t is the transmission probability of the "transparent" zones, f is the ratio of "opaque" zone transmission to "transparent" zone transmission $(\exp(-\Sigma_o D)/\exp(-\Sigma_t D))$, and N_o is the total source strength. A similar relationship can be written for a pinhole system.

$$N_o^i = (SNR)^2 \left(\frac{4S_1}{d_{PH}}\right)^2 \frac{1}{\eta_{det}} \quad (2)$$

where d_{PH} is the diameter of the pinhole.

SNR, system solid angle, and detector efficiency affect pinhole and zone plate system source strength relationships in the same way. The advantage of a zone plate over a pinhole with similar resolution is its larger solid angle. This advantage depends only on the number of zones. The resolution of a pinhole system is about the diameter of the pinhole. The resolution of a zone plate system is about twice the width of the outer zone. The diameter of a zone plate is related to the outer zone width by

$$d_{ZP} = \frac{2\Delta R_N}{\left(1-\sqrt{\frac{N-1}{N}}\right)} \quad (3)$$

Thus the ratio of zone plate system to pinhole system solid angle is

$$\left(\frac{d_{ZP}}{d_{PH}}\right)^2 = \frac{1}{\left(1-\sqrt{\frac{N-1}{N}}\right)^2} \quad (4)$$

The constant in equation 1 equals 1.23 and is due to the reconstruction coherence effects. The zone plate system relationship has three additional factors which decrease the advantage gained by the solid angle enhancement. $P_t/2$ is the fraction of source events incident on the zone plate that pass through the "transparent" zones. It represents the effective open area of the zone plate. It is for this reason that we want to maximize P_t. The factor $(1+f)/(1-f)^2$ accounts for the zone plate modulation caused by transmission through the "opaque" zones. In general the better the signal modulation the smaller the required source strength. The term N_o/N_o^i shows that the required strength of the i^{th} source element depends on the ratio of the total number of source events to the number of events in the source resolution element of interest. For a uniformly emitting source this expression is just the number of equal strength source elements.

Neutron zone plate thickness is a compromise between minimizing the required source strength and providing the required field of view. Figure 4 shows the required source strength for a point source as a function of the zone plate thickness for alternating aluminum and gold zones ($\Sigma_t = 0.1$ cm^{-1} and $\Sigma_o = 0.3$ cm^{-1}). The shape of the curve depends only on the macroscopic cross section of the zone plate materials. The minimum source strength occurs for a thickness of 9.3 cm but increases by only 10% between thicknesses of 6.7 and 12.7 cm. The required source strength is high for thin zone plates because of the poorer signal modulation. Even though the signal modulation improves for thicker zone plates, the required source strength increases because the average transmission of the zone plate is decreasing.

The neutron zone plate field of view decreases with increasing thickness. The thin zones look like collimators. Thus to achieve the widest field of view we want to minimize the zone plate thickness. For the examples shown in this paper, a 5-cm thick aluminum/gold zone plate is used. This improves the field of view over a 9.3-cm thick zone plate by 86% while increasing the required number of source events by less than 40%. Field of view is defined later.

The neutron zone plate system offers improved image detection over a pinhole system for imaging small sources because of the improved system solid angle. The diameter of a 100-zone zone plate is 200 times that of a pinhole of equivalent resolution (a solid angle increase of 40,000). Figure 5 shows the ratio of the required pinhole system source strength to the zone plate system source strength as a function of source diameter for a uniformly emitting disk source. For small sources, the zone plate system requires a factor of 1000 less source neutrons than a pinhole to achieve the same SNR. For a source diameter larger than 170-μm the source strength advantage is less than 10, and for sources larger than 540 μm the pinhole system is actually superior. Unlike a pinhole system, with a zone plate system, detected events from all source points contribute to the noise associated with the source point of interest. A zone plate offers substantial improvement for small localized sources, but can actually be a poorer choice than a pinhole for large distributed sources.

FUZZY ZONE BOUNDARIES

Zone boundaries of a zone plate look "fuzzy" to penetrating radiation originating at locations other than the zone plate focus. We use Monte Carlo techniques to study the effect of fuzzy boundaries on system characteristics like the field of view, planar resolution, tomographic resolution, quantum noise, and distributed sources. First a source distribution is selected. Point sources are used to evaluate the point spread function (PSF) as a function of system parameters. Flat uniformly emitting disks are used to look at extended sources. The position and direction for each source event is randomly selected. Then each neutron is transported through the zone plate to the detector to form the coded image. If the neutron has a collision in the zone plate, the particle is removed from the calculation. Scattered events degrade the system modulation by contributing to the uniform background of the coded image. For systems considered in this paper the change in modulation is negligible.

For this study, each computer generated coded image is numerically reconstructed on a computer. The reconstruction technique simulates the laboratory method of illuminating the coded image with a coherent laser beam. It does this by launching a spherical wave from each image point and calculating the resulting field amplitude over the source region of interest. The wave length used is just that used for an ideal zone plate system. Once the reconstructed source distribution is formed, lineouts are taken to determine quantities such as full width at half maximum (FWHM) and peak amplitude.

Field Of View

The point spread function was used to examine the field of view of thick zone plates. The PSF was determined for a point source at the focus of the zone plate and for off axis source points located in the plane perpendicular to the zone plate axis and containing the focus. Figure 6A shows the PSF peak amplitude (normalized to the point at the ZP focus) verses the source distance (in normalized units) off axis for zone plate thicknesses of 5 and 10 cm. The distance scale is plotted in units of a field of view quality parameter. This parameter is defined in the plane formed by the system axis and an off axis source point. It is the radial distance from the focus where source radiation no longer has a direct path to the image plane through the outer "transparent" zone. The amplitude decreases as the source is moved further off axis. For a normalized distance of 1, the amplitude remains fairly high (greater than 0.9) for both thicknesses. Figure 6B shows the the PSF FWHM in units of the outer zone width versus the source distance off axis. A very slight increase in the FWHM occurs between the focus point and a normalized distance of 1. For 100 zones, the FWHM is nearly independent of the absolute zone plate thickness when plotted verses the normalized source distance off axis. Based on these curves and the desire to quantify the field of view we arbitrarily define the edge of the field of view to be at a point $((S_1+D)/D)*\Delta R_N$ off axis. For greater distances than this, an image may be observed, but with a poorer SNR and spatial resolution. For the 5- and 10-cm thick zone plates the respective fields of view are 110 and 60 μm.

Figure 7 shows the PSF amplitude and FWHM versus source distance off axis for 25, 51, and 101 zones with the zone plate thickness set at 5 cm. In general the more zones used, the better the image resolution. The number of zones has a significant effect when the central zone diameter is smaller than the field of view, and relatively little effect when the field of view is smaller than the central zone diameter.

Planar Resolution (Two Point Resolution)

We wish to define a resolution standard similar to the Rayleigh criterion so that comparison with other imaging techniques may be easily made. We choose a point source pair and calculate the reconstructed intensity distribution. The point pair is considered marginally resolved when the reconstructed valley to peak ratio is 0.735, similar to the Rayleigh criterion for incoherent sources. Figure 8 shows lineouts taken through images of point source pairs at the zone plate focus and at the edge of the field of view. For points 10, 11 and 12 μm from a point at the zone plate focus, the zone plate system classically resolves two points spaced 11-μm apart. For points 10, 11 and 12 μm from a point at 53 μm off axis (at the edge of the field of view) the system resolves the points with 12-μm separation. The resolution of the ideal zone plate system (with optical reconstruction [4]) is given by

$$\delta = 1.64 \left(\frac{S_1 + S_2}{S_2}\right) \Delta R_N \qquad (5)$$

For our system the ideal resolution is $2.0\Delta R_N$. The computer simulations typically have a planar resolution of $2.2\Delta R_N$.

Depth Of Field

We studied the depth of field for zone plate systems by examining the PSF for points along the system axis. For a 100-zone, 5-cm-thick zone plate with a 5-μm outer zone width, points within $S_1(S_1+D)/2ND$ of the zone plate focus produce a good quality PSF. This distance is the Z-axis position at which source radiation no longer has a direct path through the outer "transparent" zone to the image plane. We use this distance to signify the edge of the depth of field. For systems with S_1 distances between 25 and 200 cm and a magnification of 6, the PSF amplitude for points at the edge of the field have 75 to 90% of the amplitude for points at the system focus. The PSF FWHM increases by less than 10%. For the zone plate system used in Fig. 6 the depth of focus extends 2.75 cm on either side of the zone plate focus.

Tomographic Resolution

The effect of thick zone plates on tomographic resolution is examined by looking at the PSF of a point source reconstructed in various axial planes. A measure of the tomographic capability of a zone plate system is the distance in source space to the first null in the intensity distribution [4]. For a thin zone plate, this occurs at a value of

$$\Delta = \frac{S_1}{N} \frac{(S_1+S_2)}{S_2} \quad . \tag{6}$$

This equation is useful as a tomographic figure of merit. The peak to null distances measured in Monte Carlo simulations of the system described in Fig. 6 with an S_1 distance of 50 cm are 0.65 cm for a point at the focus and 0.75 cm for a point at the edge of the depth of field. These values agree well with the calculated value of 0.6 for this sytem.

DETECTOR ELEMENT SIZE

Different coded image recording media are possible. It might be scintillator arrays, film, or track detectors. Each system has a spatial resolution associated with the detection of an event. We have examined the effect of detector resolution on zone plate imaging by calculating the PSF for systems with detector arrays with different size elements. Figure 9 shows the PSF peak amplitude and FWHM versus detector element size. The element dimension is plotted in units of the outer zone width times the system magnification. For values less than 1 the system performs nearly as well as if the exact position of each event were known. At 1, the amplitude has decreased to 90% and the FWHM shows no change. Above a value of 2, the amplitude and FWHM begin to deteriorate rapidly. The system design for our Nova example has a magnification of 6. Thus a 400 by 400 element array of 30-μm square detector elements would be adequate. The SNR will be about 10% less than for the perfect system. It should be noted that the required number of detector elements to achieve a specified system resolution is dependent only on the number of zones in the zone plate.

CONCLUSION

We have examined the use of a zone plate to image penetrating radiation such as 14-MeV neutrons. Calculations indicate that it may be possible to produce high quality images of neutron source distributions using a thick zone plate made of alternating layers of "transparent" and "opaque" materials such as aluminum and gold. The zone plate must be thick to optimize the zone plate modulation, and it must be tapered so that it approximates an ideal zone plate to sources within its field of view and depth of field.

The primary effect of the thick zone plate is to cause the image of the zone boundaries to appear fuzzy in the coded image for events coming from points other than the zone plate focus. We have found that the zone plate causes little distortion of the PSF for source points $((S_1+D)/D)*\Delta R_N$ off axis. Thus we have defined the field of view for a zone plate as twice this value. The PSF distortion is nearly independent of the number of zones in the zone plate if the field of view is smaller than the central zone of the zone plate. For images within this field of view, the image characteristics such as planar and tomographic resolution are quantitatively nearly identical to the values calculated for a thin zone plate. For a field of view greater than the central zone, the PSF distortion depends on the number of zones.

We demonstrated a numerical reconstruction procedure. In the past, all our zone plate work used laboratory reconstruction where the coded image is illuminated with laser light to form an image on film. In this work we reconstruct the source distribution from the computer simulated coded images using numerical techniques.

The zone plate has tremendous potential to enhance collection efficiency over a pinhole system with similar distances and resolution. With 100 zones the zone plate has a solid angle 40,000 times greater than a pinhole system with equivalent resolution and similar dimensions. The zone plate has a significant advantage over a pinhole for small localized sources but provides little advantage over (and indeed may not be as good as) a pinhole system for imaging distributed sources that are larger than the central zone plate zone.

REFERENCES

1. N. M. Ceglio and L. W. Coleman, "Spatially Resolved Emission from Laser Fusion Targets," Phys. Rev. Lett., 39:20 (1977).
2. D. T. Attwood, N. M. Ceglio, E. M. Campbell, J. T. Larson, D. M. Matthews, and S. M. Lane, "Compression Measurement in Laser Driven Implosion Experiments," in: "Laser Interaction and Related Plasma Phenomena," H. Schwarz et. al., eds, (Plenum, New York, 1981), Vol. 5, pp. 435-438.
3. R. A. Lerche and G. E. Sommargren, "Collimator Design for Neutron Imaging," Laser Program Annual Report - 1981, pp. 5-33 to 5-37; UCRL-50021-81.
4. N. M. Ceglio and D. W. Sweeney, "Zone Plate Coded Imaging: Theory and Applications", in: "PROGRESS IN OPTICS," E. Wolf ed, (North-Holland Physics Publishing, 1984) vol XXI, pp. 289-354.
5. A Fresnel zone plate coded aperture is a series of alternating transparent and opaque equi-area annular rings.
6. D. Rudolph and G. Schmahl, "High Power Zone Plates for a Soft X-Ray Microscope," in: "Ultrasoft X-ray Microscopy: Its Application to Biological and Physical Systems," D. F. Parsons, ed., New York Academy of Sciences, New York (1980).
7. K. A. Nugent and B. Luther-Davies, "Application of Penumbral Imaging to Thermonuclear Neutrons," J. Appl. Phys. 58:2508 (1985).

FIGURE CAPTIONS

Fig. 1. Zone plate coded imaging is a two step process. Radiation from the source casts a shadow of the Fresnel zone plate onto a recording media to form a coded image. The coded image is typically unfolded by illuminating a transparency of the shadowgraph with coherent light from a laser.

Fig. 2. A neutron zone plate is thick and tapered.

Fig. 3. An ideal zone plate transfer function has 100% modulation with sharp zone boundaries. A 5-cm thick zone plate made of alternating aluminum and gold layers has a 46% modulation and sharp zone boundaries for points near the focus. Zone boundaries become fuzzy for source points away from the focus.

Fig. 4. The optimum neutron zone plate thickness is a compromise between minimizing the required source strength and providing the required field of view. The curves are plotted for a 100 zone aluminum/gold zone plate system with a 5-μm outer zone width looking at a point source with $S_1 = 50$ cm, $S_2 = 250$ cm, and a detector efficiency of 1%. (--- source neutrons, -.-. field of view, —— detected neutrons.)

Fig. 5. The ratio of pinhole system source strength to zone plate system source strength to obtain equivalent images depends on the source size and the zone plate characteristics. This curve shows the advantage of a 100 zone, 5-cm thick, 5-μm outer zone aluminum/gold zone plate over a 11-μm diameter pinhole versus source diameter for a uniformly emitting disk. For source diameters greater than 170 μm the advantage is less than a factor of 10, for diameters greater than 540 μm the pinhole has an advantage over the zone plate.

Fig. 6. We define field of view as the radial distance α from the zone plate focus where a particle no longer has a direct path to the image plane through the outer zone. The PSF amplitude and FWHM show little deterioration for distances less than α. These curves are for 100 zone, 5 and 10-cm thick, aluminum/gold zone plates with 5-μm outer zone widths 50 cm from the source. The image plane is 250 cm from the zone plate.

Fig. 7. The PSF amplitude and FWHM show some dependence on the number of zones. Significant deterioration for radial distances less than α occur when the central zone radius is less than α. These curves are for the 5-cm thick zone plate system of figure 6.

Fig. 8. Lineouts taken through images of source point pairs located at the focus and at the edge of the field of view for 5-cm thick zone plate system of figure 6. The zone plate resolves two point sources 11-μm apart at the focus and 12-μm apart at the edge of the field of view.

Fig. 9. PSF peak amplitude and FWHM versus detector element size for the 5-cm thick zone plate system of figure 6. Square detector elements with side lengths less than the outer zone width times the system magnification (M) cause only very slight deterioration in the system quality.

2074G / 0099G

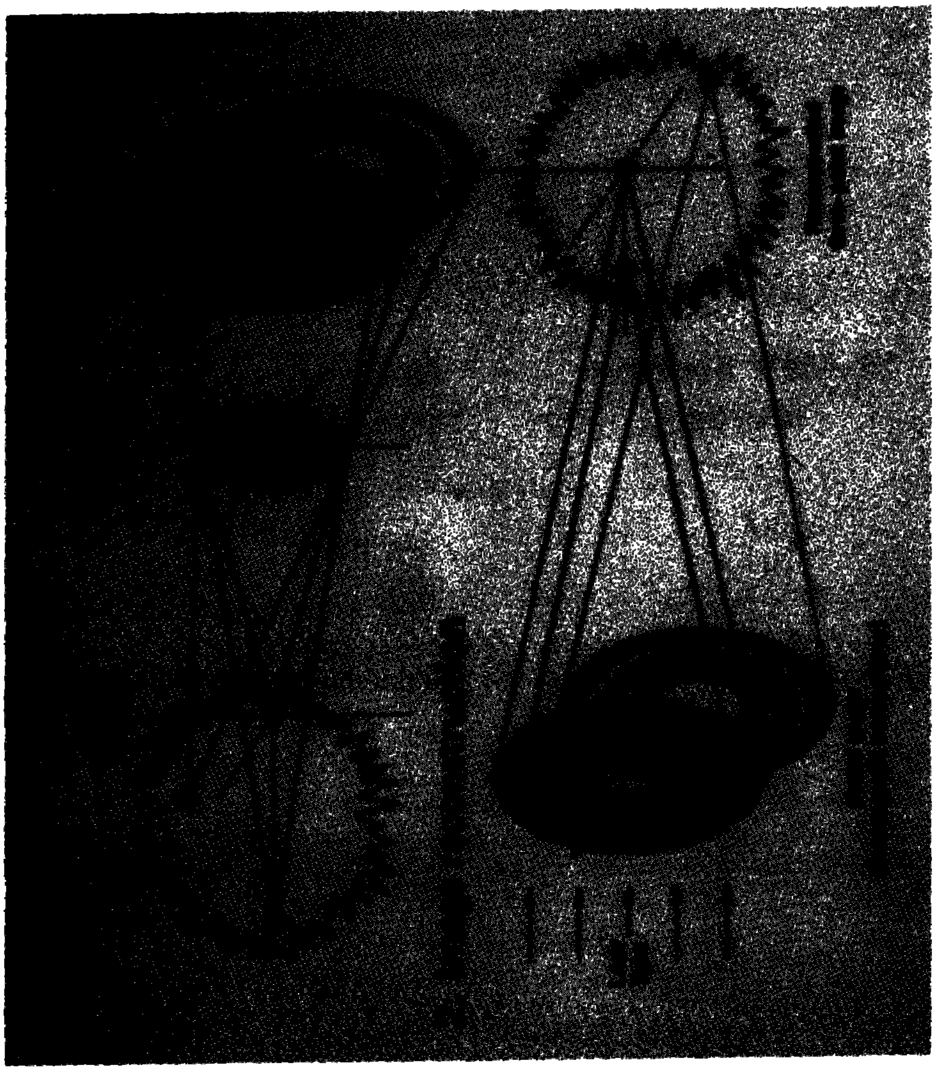

Fig. 1

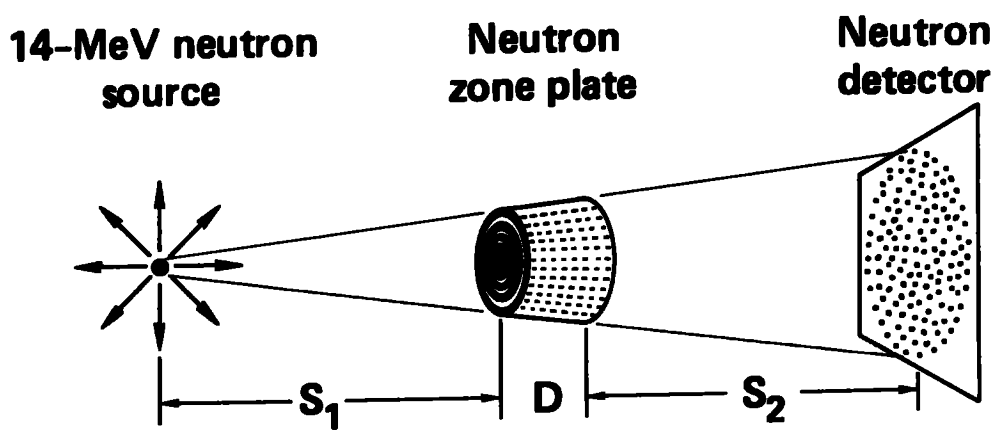
14-MeV neutron
source
Neutron
zone plate
Neutron
detector
S1
D
S2

Fig. 2

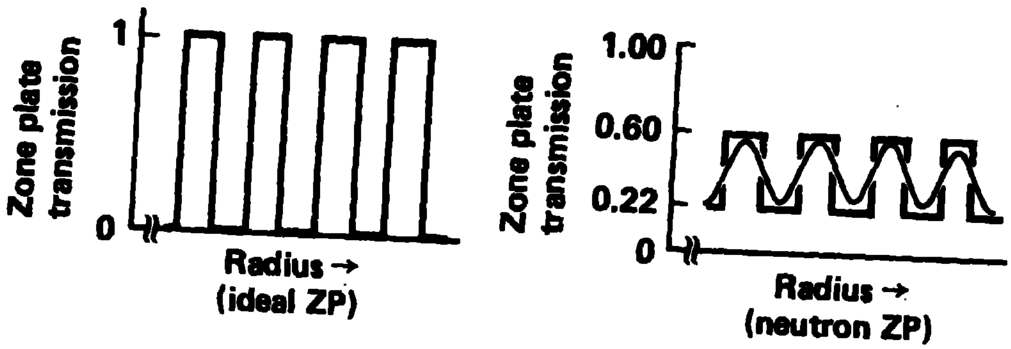
Zone plate transmission
1
0
Radius →
(ideal ZP)
Zone plate transmission
1.00
0.60
0.22
0
Radius →
(neutron ZP)

Fig. 3

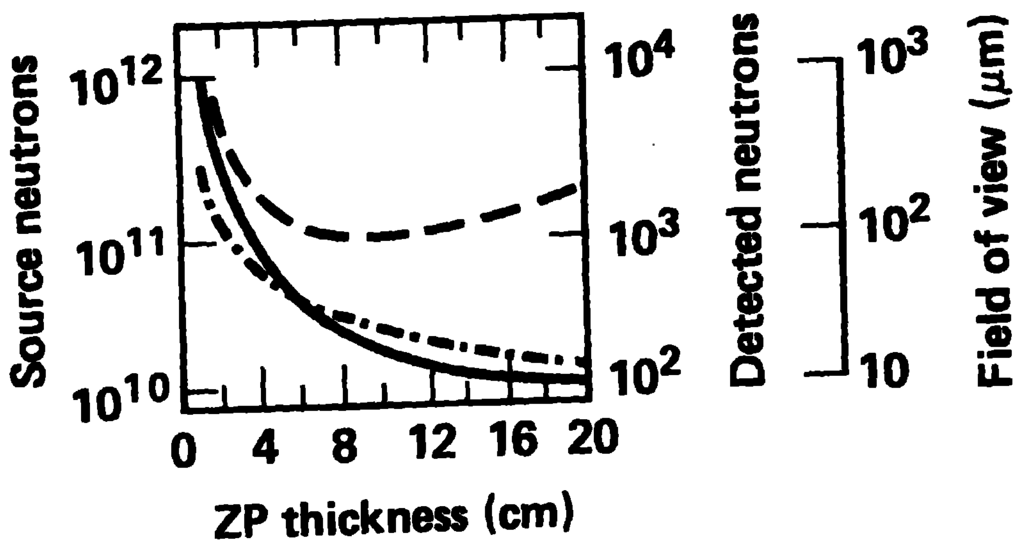
Source neutrons
10^{12}
10^{11}
10^{10}
0 4 8 12 16 20
ZP thickness (cm)
10^4
10^3
10^2
Detected neutrons
10^3
10^2
10
Field of view (μm)

Fig. 4

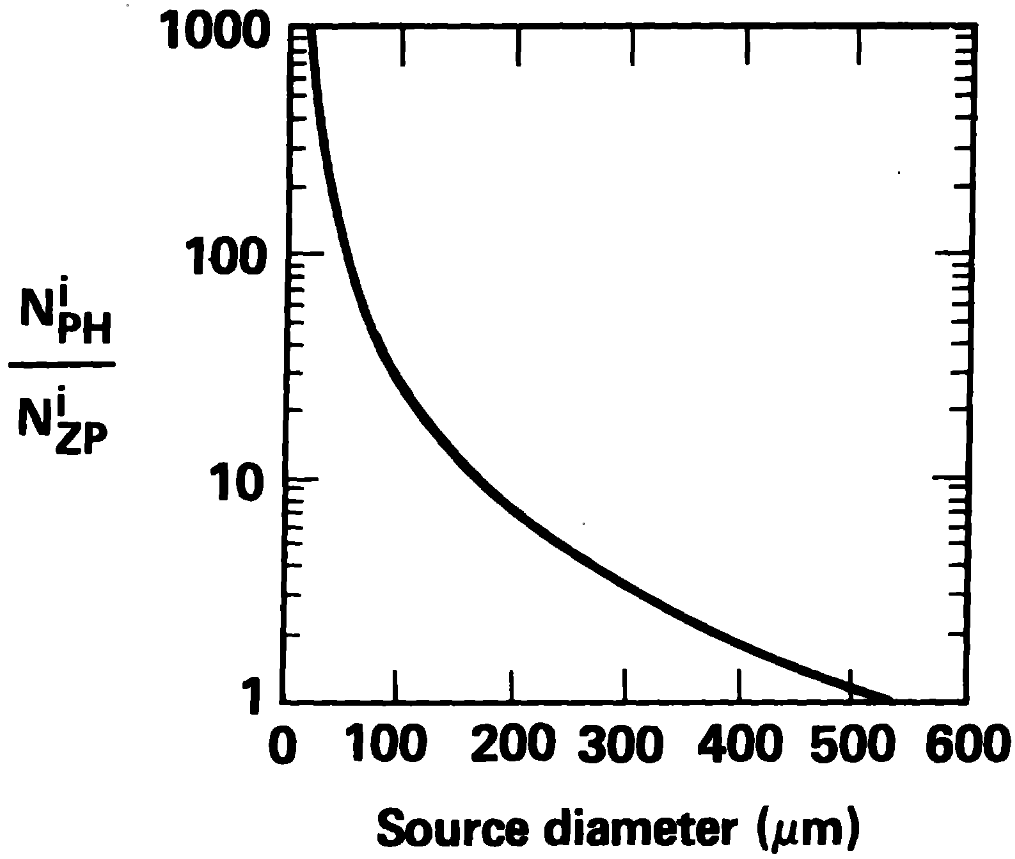

1000
100
10
1
N^i_{PH} / N^i_{ZP}
0
100
200
300
400
500
600
Source diameter (μm)

Fig. 5

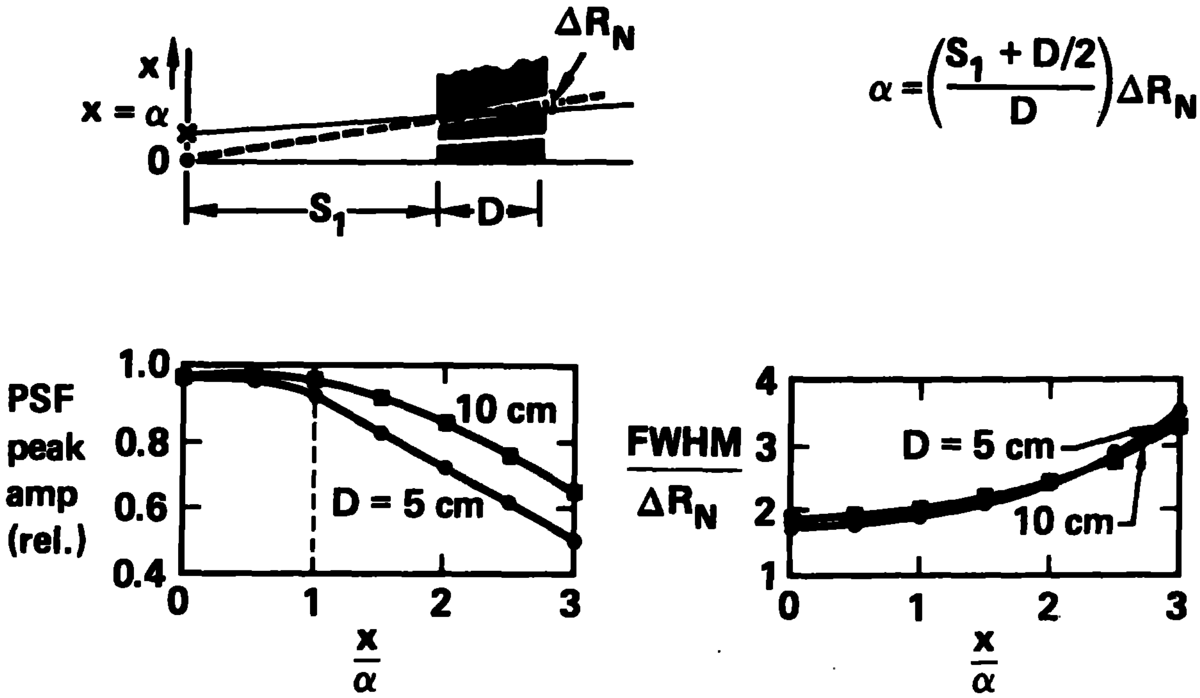

ΔR_N
x
x = α
0
S_1
D
α = ((S_1 + D/2)/D) ΔR_N
PSF peak amp (rel.)
1.0
0.8
0.6
0.4
10 cm
D = 5 cm
0
1
2
3
x/α
FWHM/ΔR_N
4
3
2
1
D = 5 cm
10 cm
0
1
2
3
x/α

Fig. 6

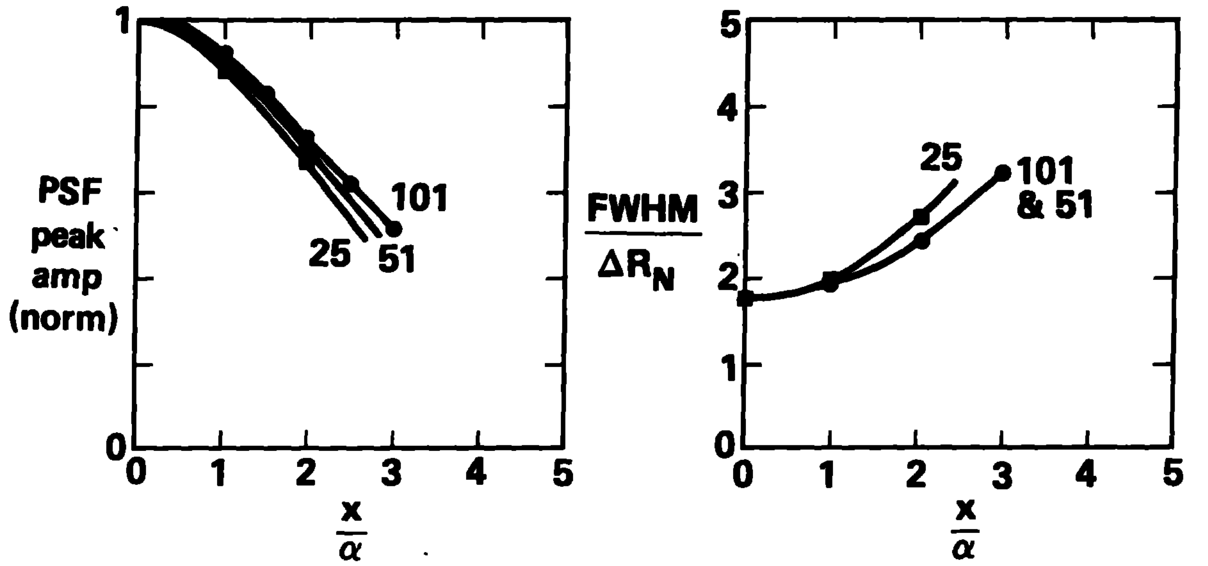
PSF
peak
amp
(norm)
1
0
0
1
2
3
4
5
x/α
101
25
51
FWHM/ΔR_N
5
4
3
2
1
0
0
1
2
3
4
5
x/α
25
101
& 51

Fig. 7

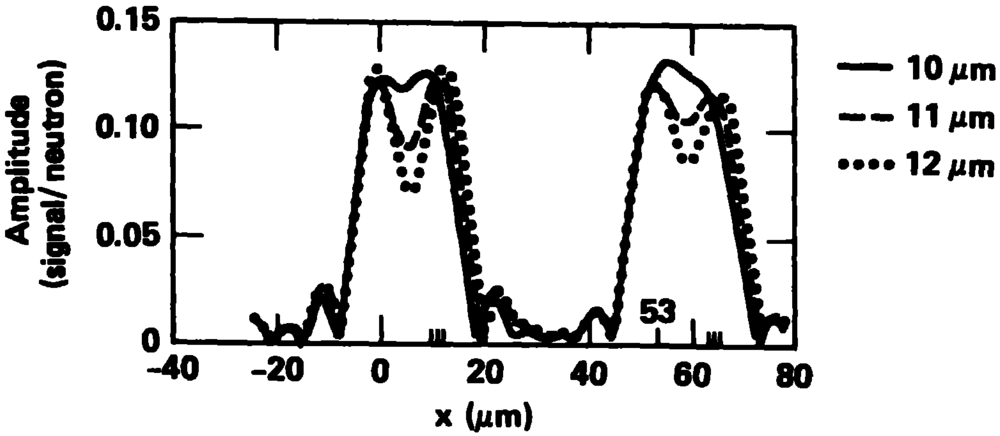
Amplitude (signal/neutron)
0.15
0.10
0.05
0
-40
-20
0
20
40
60
80
x (μm)
53
10 μm
11 μm
12 μm

Fig. 8

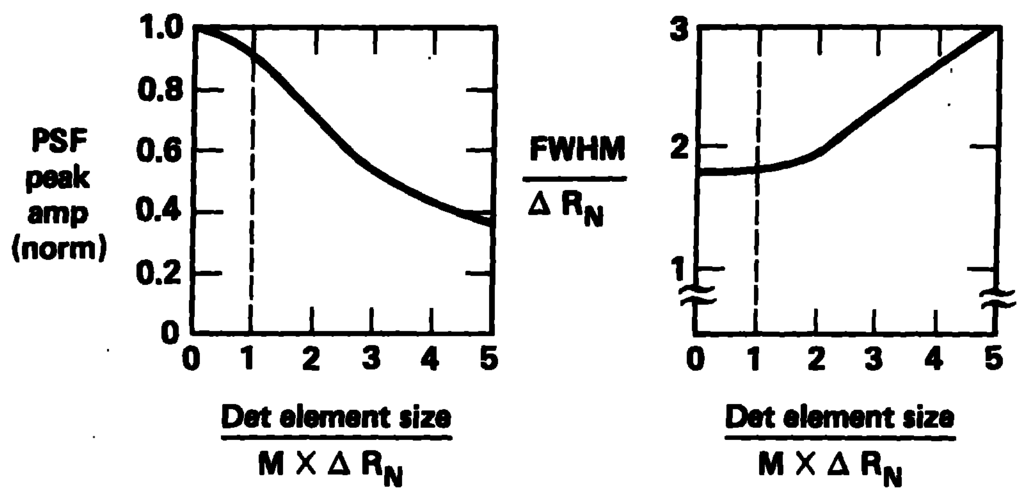
PSF
peak
amp
(norm)
1.0
0.8
0.6
0.4
0.2
0
0 1 2 3 4 5
Det element size
M X Δ R_N
FWHM
Δ R_N
3
2
1
0 1 2 3 4 5
Det element size
M X Δ R_N

Fig. 9